Multivalency enables unidirectional switch-like competition between intrinsically disordered proteins

Rebecca B. Berlow[a,b], H. Jane Dyson[a,b], and Peter E. Wright[a,b,1]

[a]Department of Integrative Structural and Computational Biology, The Scripps Research Institute, La Jolla, CA 92037; and [b]Skaggs Institute for Chemical Biology, The Scripps Research Institute, La Jolla, CA 92037

Contributed by Peter E. Wright; received September 20, 2021; accepted November 22, 2021; reviewed by David Eliezer and Julie Forman-Kay

Intrinsically disordered proteins must compete for binding to common regulatory targets to carry out their biological functions. Previously, we showed that the activation domains of two disordered proteins, the transcription factor HIF-1α and its negative regulator CITED2, function as a unidirectional, allosteric molecular switch to control transcription of critical adaptive genes under conditions of oxygen deprivation. These proteins achieve transcriptional control by competing for binding to the TAZ1 domain of the transcriptional coactivators CREB-binding protein (CBP) and p300 (CREB: cyclic-AMP response element binding protein). To characterize the mechanistic details behind this molecular switch, we used solution NMR spectroscopy and complementary biophysical methods to determine the contributions of individual binding motifs in CITED2 to the overall competition process. An N-terminal region of the CITED2 activation domain, which forms a helix when bound to TAZ1, plays a critical role in initiating competition with HIF-1α by enabling formation of a ternary complex in a process that is highly dependent on the dynamics and disorder of the competing partners. Two other conserved binding motifs in CITED2, the LPEL motif and an aromatic/hydrophobic motif that we term ϕC, function synergistically to enhance binding of CITED2 and inhibit rebinding of HIF-1α. The apparent unidirectionality of competition between HIF-1α and CITED2 is lost when one or more of these binding regions is altered by truncation or mutation of the CITED2 peptide. Our findings illustrate the complexity of molecular interactions involving disordered proteins containing multivalent interaction motifs and provide insight into the unique mechanisms by which disordered proteins compete for occupancy of common molecular targets within the cell.

protein–protein interaction | binding motif | allostery | hypoxic response | transcriptional regulation

Intrinsically disordered proteins (IDPs) are abundant in eukaryotes and play crucial roles in cellular signaling and regulation (1). To maintain fidelity of cellular signaling in response to varied stimuli, IDPs compete for binding of common molecular interaction hubs with surprising efficiency. Numerous experimental and computational studies (reviewed in refs. 1–5) have characterized IDP binding processes in great detail, contributing to a growing body of knowledge that illustrates how IDPs utilize their unique physicochemical properties to recognize their molecular targets. Many IDPs contain multiple discrete binding motifs that function synergistically to enable multivalent interactions with their molecular partners. IDP binding reactions are complex and often proceed through multistep processes that allow for partial engagement of the IDP with a binding partner via one or more binding motifs, prior to adopting the final bound state. However, disordered proteins are also highly represented in protein–protein interaction networks that are characterized by "many-to-one" binding interactions, where many different IDPs compete for binding sites on molecular targets that may be already occupied by other ligands (6). One can speculate that in the case of an IDP competing for a shared binding site, disorder and flexibility, as well as the ability to partially engage binding partners that are already occupied by other ligands through selective interactions of one or more binding motifs, would be extremely advantageous.

The general transcriptional coactivator CREB (cyclic-AMP response element binding protein)-binding protein (CBP) is an excellent model for understanding competition of IDPs for shared binding sites. CBP and its paralog p300 play indispensable roles in numerous cellular processes and function as key integrators of signal transduction pathways (7). CBP and p300 bind a wide array of intrinsically disordered transcription factors and transcriptional regulatory proteins (7–10), predominantly through interactions with their folded protein interaction domains (1, 11). The folded TAZ1 domain is the binding site for the disordered regions of transcription factors and transcriptional regulators that control stress response pathways in the cell, including the hypoxia-inducible transcription factor HIF-1α and its negative feedback regulator CITED2 (12–14). Under conditions of oxygen deficiency, HIF-1α interacts with TAZ1 via its intrinsically disordered C-terminal transactivation domain (CTAD) to drive transcription of critical adaptive genes (12, 15). One such gene encodes the protein CITED2, which functions as a negative feedback regulator of HIF transcriptional activity by directly competing with HIF-1α for binding to TAZ1 (13).

Previously, we showed that CITED2 displaces HIF-1α from its complex with TAZ1 with switch-like efficiency in a

Significance

Intrinsically disordered proteins must frequently compete for binding to shared interaction hubs to perform their cellular functions. Here, we describe the mechanism by which two disordered proteins that regulate the transcriptional response to hypoxia compete for binding to the folded TAZ1 domain of the transcriptional coactivators CBP and p300. CITED2, a negative feedback regulator of HIF-1α, displaces HIF-1α from TAZ1 in a unidirectional, switch-like manner. Efficient competition for binding of the TAZ1 domain is highly dependent on the flexibility and multivalency of the HIF-1α and CITED2 activation domains. Differences in the strength of coupling of the CITED2 and HIF-1α binding motifs are key determinants of unidirectionality and underscore the role of multivalency in regulation of cellular processes by disordered proteins.

Author contributions: R.B.B., H.J.D., and P.E.W. designed research; R.B.B. performed research; R.B.B., H.J.D., and P.E.W. analyzed data; and R.B.B., H.J.D., and P.E.W. wrote the paper.

Reviewers: D.E., Weill Cornell Medicine; J.F.-K., Hospital for Sick Children.

The authors declare no competing interest.

[1]To whom correspondence may be addressed. Email: wright@scripps.edu.

This article contains supporting information online at http://www.pnas.org/lookup/suppl/doi:10.1073/pnas.2117338119/-/DCSupplemental.

Published January 10, 2022.

unidirectional allosteric process that relies on the flexibility of both HIF-1α and CITED2 as well as the conformational plasticity of TAZ1 (16–18). Solution structures of the HIF-1α:TAZ1 and CITED2:TAZ1 complexes show that the intrinsically disordered activation domains of HIF-1α and CITED2 fold to form helical structure upon binding to TAZ1 (Fig. 1*A*) (19–22). HIF-1α and CITED2 are both prototypical examples of IDPs that participate in multivalent interactions mediated by discrete binding motifs. HIF-1α and CITED2 both contain a conserved four-residue LP(Q/E)L motif that binds in the same site and orientation to TAZ1. HIF-1α forms three helices (αA, αB, αC) that are connected by flexible linkers, with the LPQL motif located just N-terminal to the start of the αB helix (19, 20). CITED2 interacts with TAZ1 through an N-terminal helical region (αA), the LPEL motif, and a region containing conserved hydrophobic and negatively charged amino acids, which we term the ϕC motif, located immediately C-terminal to LPEL (Fig. 1*B*) (21, 22). Our previous work demonstrated that the αA helix of HIF-1α remains highly dynamic in the complex with TAZ1, allowing access for the CITED2 αA helix to interact with its partially overlapping binding site (16, 17). Kinetic data indicate that CITED2 competes with HIF-1α by an associative mechanism in which CITED2 forms a ternary complex with HIF-1α and TAZ1 prior to HIF-1α dissociation (16). A truncated CITED2 peptide that contains the αA region but lacks the LPEL and ϕC motifs (CITED 216-242) can bind to the TAZ1:HIF-1α complex without requiring dissociation of HIF-1α (16). Taken together, these results suggest that ternary complex formation is an essential component of the switch-like competition observed between HIF-1α and CITED2. However, a detailed mechanistic understanding of the molecular determinants for unidirectional competition between HIF-1α and CITED2 for TAZ1 has not yet been described.

Our prior observations suggest that the various interaction motifs of CITED2 function synergistically to compete with HIF-1α for occupancy of TAZ1. To assess the role of the individual binding motifs in modulating the multivalent interactions of CITED2 with TAZ1 and its ability to compete with HIF-1α, we designed a series of variant CITED2 peptides in which the CITED2 transactivation domain is truncated N- or C-terminal to the LPEL motif (CITED 216-242 and CITED 216-246, respectively), as well as a peptide in which the nonproline residues of the LPEL motif are mutated to alanine (CITED APAA). These modifications have marked effects on both binding and competition, yielding critical insights into the mechanism by which CITED2 competes with HIF-1α for TAZ1 and revealing the key determinants for unidirectional switch-like competition.

Results

Contributions of CITED2 Interaction Motifs to TAZ1 Binding. The CTAD of CITED2 contains three interaction motifs (αA, LPEL, and ϕC). To evaluate the role of each of the motifs in the mechanism of the unidirectional switch, we designed a series of truncated and mutated CITED2 peptides in which the N-terminal region of the CITED2 CTAD is preserved, but the presence of the LPEL motif and/or the C-terminal region of the peptide is varied (Fig. 1*B*). For the CITED APAA peptide, we mutated the nonproline residues of the LPEL motif to alanine (retaining the αA and ϕC motifs as well as the C-terminal portion of the peptide beyond the ϕC motif). For the CITED 216-242 peptide, the CITED2 sequence was truncated N-terminal to the LPEL motif (retaining only the αA motif), whereas for the CITED 216-246 peptide, the sequence was truncated C-terminal to LPEL (retaining the αA and LPEL motifs). We note that residues C terminal to the ϕC motif are dynamically disordered and are not required for TAZ1 binding (13, 17). Together with the full-length CITED2 CTAD (CITED 216-269), these peptides provide a molecular tool kit for exploring the role of the LPEL and ϕC motifs in modulating TAZ1 binding and competition against HIF-1α.

Binding of the CITED2 peptides to TAZ1 was assayed using fluorescence anisotropy competition experiments, in which the unlabeled CITED2 peptides were titrated into a preformed

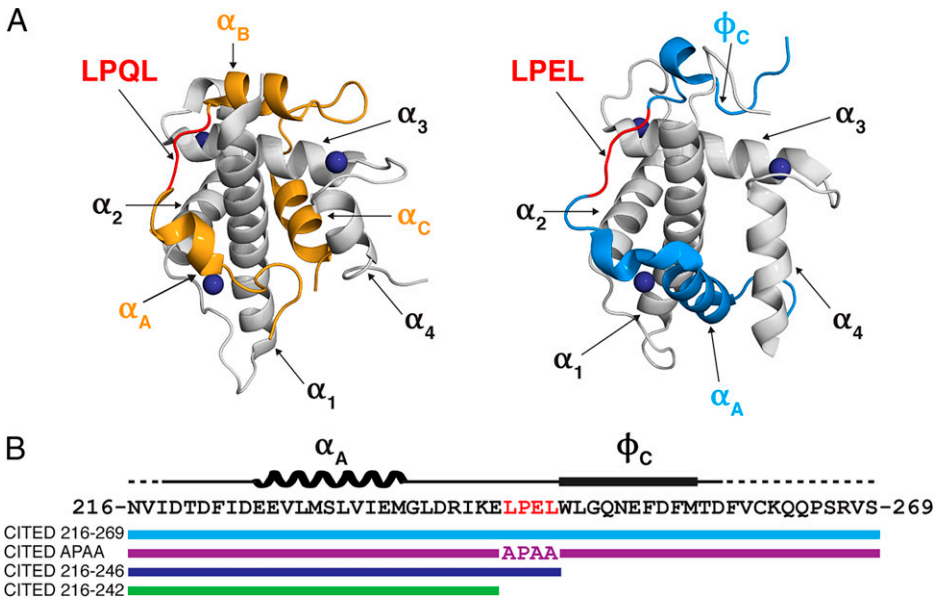

Fig. 1. Complexes and peptides included in this study. (*A*) The lowest-energy NMR structure of the CBP TAZ1 domain (gray) is shown in complex with the C-terminal activation domain of HIF-1α (residues 776 to 826; in orange; *Left*) or CITED2 (residues 220 to 259; light blue; *Right*). The LP(Q/E)L motif is highlighted in red. Labels for structural elements and binding motifs are shown in black for TAZ1, orange for HIF-1α, and light blue for CITED2. Zinc atoms are shown as dark blue spheres. Residues 260 to 269 of CITED2 are disordered and are omitted for clarity. These structural models were generated using PyMOL from Protein Data Bank ID codes 1L8C and 1R8U. (*B*) The amino acid sequence for the CITED2 CTAD (residues 216 to 269), with the LPEL motif highlighted in red. A cartoon representation of the CITED2 peptide and key binding motifs is shown above the sequence. The dashed lines represent regions of the peptide that remain disordered in complex with TAZ1. The variant peptides are illustrated as colored bars below the sequence.

Table 1. K_d^{app} values for CITED2 peptides from fluorescence competition assays

	K_d^{app}	
Competitor	A594–CITED2	A594–HIF-1α
CITED 216–269	10 ± 1 nM*	0.2 ± 0.1 nM*
CITED 216–246	5 ± 1 μM	210 ± 20 nM
CITED 216–242	36 ± 10 μM*	1.1 ± 0.3 μM
CITED APAA	2.5 ± 0.2 μM†	50 ± 10 nM†

Data are shown for competition with a preformed complex of Alexa594-labeled CITED2 or Alexa594-labeled HIF-1α and TAZ1. The reported K_d^{app} values and associated uncertainties represent the average and SD of the fitted K_d^{app} values from at least three independent measurements.

*Values were previously reported by Berlow et al. (16).

†Values were previously reported by Usui-Ouchi et al. (23).

complex of Alexa594–CITED 216-269 and TAZ1. The apparent K_d (K_d^{app}) values for the truncated and mutated CITED2 peptides demonstrate the importance of the LPEL and ϕC motifs for forming stable complexes with TAZ1 (Table 1 and *SI Appendix*, Fig. S1). Mutation of the LPEL motif (CITED APAA) and truncation of CITED2 to remove the ϕC motif and C-terminal region (CITED 216-246) weaken the apparent affinity for TAZ1 by 250- and 500-fold, respectively, relative to the K_d^{app} for CITED 216-269 (16, 23). Deletion of both the LPEL and ϕC motifs, in the CITED 216-242 peptide, further destabilizes the interaction with TAZ1, with a K_d^{app} that is more than three orders of magnitude larger than that of CITED 216-269 (16).

Solution NMR spectroscopy was used to characterize the binding of the various CITED2 peptides to ^{15}N-TAZ1 (Fig. 2 and *SI Appendix*, Figs. S2–S4). The truncated (CITED 216-246 and CITED 216-242) and mutated (CITED APAA) peptides cause chemical shift changes in TAZ1 that are similar to those caused by binding of the full-length CITED2 CTAD (CITED 216-269) (16, 21); >80% of the resonances in the ^{1}H-^{15}N heteronuclear single-quantum coherence (HSQC) spectra of ^{15}N-TAZ1 bound to the various CITED2 peptides could be assigned by comparison with the assigned spectrum of the ^{15}N-TAZ1:CITED 216-269 complex (21). The weighted average ^{1}H, ^{15}N chemical shift differences between TAZ1 cross-peaks in the free and CITED2 peptide-bound states reveal that the binding mode of each of the CITED2 peptides is largely conserved (*SI Appendix*, Fig. S5). Binding of the CITED2 peptides has the largest effect on resonances arising from residues in the TAZ1 α1 and α4 helices, which form the main contact surface for the CITED2 αA helix (Fig. 1). Further, comparison of the spectra of ^{15}N-TAZ1 bound to the variant peptides and to CITED 216-269 highlights that the largest variation in chemical shift is for the residues at the N-terminal ends of the TAZ1 α1 and α3 helices and the linker between the TAZ1 α2 and α3 helices (*SI Appendix*, Fig. S5 *D–F*). These regions of TAZ1 form the contact surface for the CITED2 LPEL motif and thus, would be expected to exhibit different chemical shifts in the presence of the truncated and mutated CITED2 peptides.

Contribution of CITED2 Motifs to Competition with HIF-1α. The NMR data demonstrate that the variant CITED2 peptides bind to TAZ1 in a similar manner, although more weakly, even when important binding motifs are missing. However, to act as a negative regulator of the hypoxic response, CITED2 must compete with HIF-1α for TAZ1 binding. All of the variant peptides include the CITED2 αA region but are missing one or more of the other CITED2 binding motifs. To assess the contribution of the CITED2 LPEL and ϕC motifs to the ability of the CITED2 peptides to compete with HIF-1α for TAZ1, we used fluorescence anisotropy competition experiments where the CITED2 variant peptides were titrated into a preformed complex of Alexa594-labeled HIF-1α peptide and unlabeled TAZ1. The truncated and mutated peptides are deficient in competing against HIF-1α relative to the full-length CITED 216-269 peptide (Fig. 3). The CITED 216-242 peptide, lacking both the LPEL and ϕC motifs, is the worst competitor, with a K_d^{app} more than three orders of magnitude weaker than that of CITED 216-269 (Fig. 3 and Table 1). Truncation of CITED2 C-terminal to the LPEL motif (CITED 216-246) also has marked effects on the ability to compete with HIF-1α, suggesting that the aromatic and hydrophobic residues in the ϕC motif that make stabilizing interactions with the TAZ1 domain also play a role in promoting competition with HIF-1α. The CITED APAA peptide, which retains the ϕC motif but is mutated at the nonproline residues of the LPEL motif, is the least deficient in its ability to displace HIF-1α from its complex with TAZ1, albeit with a K_d^{app} that is still two orders of magnitude weaker than that of CITED 216-269.

Further insights were obtained using NMR titrations. HIF-1α is fully displaced from its complex with TAZ1 by equimolar concentrations of CITED 216-269 (Fig. 4*A*), whereas the truncated CITED2 peptide lacking the LPEL and ϕC motifs (CITED 216-242) is unable to displace HIF-1α except at much higher concentrations (Fig. 4*B* and *SI Appendix*, Fig. S6) (16). The spectral changes upon addition of one, three, or five molar equivalents of CITED 216-242 to a ^{15}N-TAZ1:HIF-1α NMR

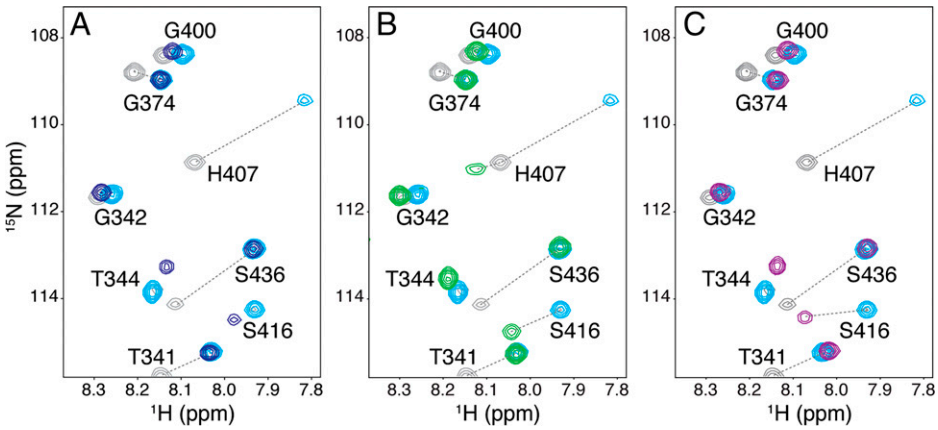

Fig. 2. The CITED2 peptides bind similarly to TAZ1. Selected regions of superimposed ^{1}H-^{15}N HSQC spectra of ^{15}N-TAZ1 (gray), ^{15}N-TAZ1 bound to CITED 216-269 (light blue), ^{15}N-TAZ1 bound to CITED 216-246 (blue; in *A*), ^{15}N-TAZ1 bound to CITED 216-242 (green; in *B*), or ^{15}N-TAZ1 bound to CITED APAA (purple; in *C*).

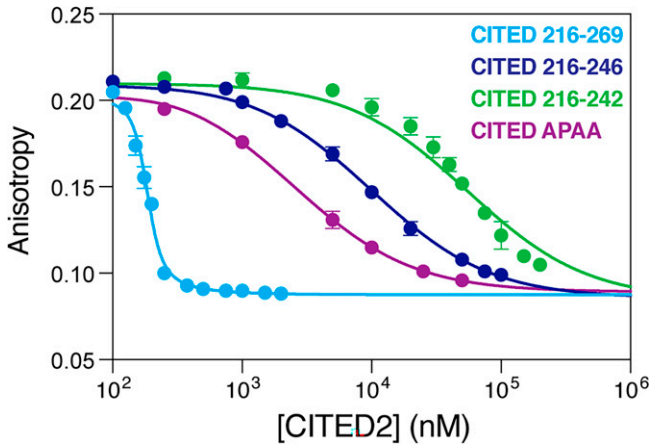

Fig. 3. Truncation and mutation of the CITED2 peptides attenuate competition between CITED2 and HIF-1α for TAZ1. Fluorescence anisotropy data for titration of CITED 216-269 (light blue), CITED 216-246 (blue), CITED 216-242 (green), and CITED APAA (purple) peptides into a preformed complex of AlexaFluor 594-labeled HIF-1α and TAZ1. Data points and error bars represent the mean and SD of at least three independent measurements. Solid lines represent the results of nonlinear least squares fitting (*Materials and Methods*).

sample (gold, orange, and magenta spectra, respectively, in Fig. 4*B*) indicate that the CITED2 αA region binds to its cognate site on TAZ1 but that HIF-1α remains bound (16). Additional NMR titration experiments, in which increasing amounts of the CITED 216-246 or CITED APAA peptides were added to NMR samples of the ^{15}N-TAZ1:HIF-1α complex, show similar behavior to CITED 216-242 (Fig. 4 *C* and *D* and *SI Appendix*, Figs. S7 and S8). The mutated or truncated peptides all show a similar pattern of chemical shift changes for TAZ1 resonances in the cognate binding site for the CITED2 αA region, which shift in fast exchange as the concentration of CITED2 peptide is increased (Fig. 4 *B–D* and *SI Appendix*, Figs. S6–S9). For the CITED 216-246 and CITED APAA peptides, we also observe an additional set of peaks that are in slow exchange with the ^{15}N-TAZ1:HIF-1α resonances and appear at positions corresponding to resonances of the ^{15}N-TAZ1:CITED2 complex. These cross-peaks increase in intensity as a function of the CITED2 peptide concentration, and there is a concomitant decrease in intensity of the resonances that are at or slightly shifted from the positions corresponding to the ^{15}N-TAZ1:HIF-1α resonances (Fig. 4 *B–D* and *SI Appendix*, Fig. S10). A modest decrease in intensity for the ^{15}N-TAZ1:HIF-1α resonances is also observed at higher concentrations of CITED 216-242 (Fig. 4*B* and *SI Appendix*, Fig. S10), even though the cross-peak at the position of the ^{15}N-TAZ1:CITED2 complex is barely detectable.

In contrast to the similarities observed in the pattern of chemical shift changes (Fig. 4 *B–D* and *SI Appendix*, Figs. S6–S9), the intensity changes in the titration spectra differ for the various CITED2 peptides. At a given CITED2 peptide concentration, the resonances that appear at the position of the ^{15}N-TAZ1:CITED2 peptide complex are more intense for CITED2 peptides with higher affinity (smaller K_d^{app} values) (Figs. 3 and 4 and Table 1). For the experiments with CITED 216-269, for which we obtain the smallest K_d^{app} value, the CITED2 bound state is fully occupied at equimolar concentrations of HIF-1α and CITED2 (Fig. 4*A*). In contrast, in the competition experiments with CITED 216-242, which has the largest K_d^{app} value, the CITED2 bound state is only weakly populated in the presence of HIF-1α and is barely detectable at even a fivefold molar excess of CITED 216-242 relative to HIF-1α and TAZ1 (Fig. 4*B* and *SI Appendix*, Fig. S10). The CITED 216-246 and CITED APAA peptides show roughly similar relative intensities of the resonances for the CITED2 bound state (Fig. 4 *C* and *D*), which is largely consistent with the intermediate K_d^{app} values for these peptides determined from the fluorescence anisotropy measurements. Taken together, these data strongly suggest that binding of the CITED2 αA motif to the TAZ1:HIF-1α complex, in a region of TAZ1 where HIF-1α makes only transient interactions (17), is the initial event in formation of the ternary ^{15}N-TAZ1:HIF-1α:CITED2 intermediate that promotes displacement of HIF-1α. Further, the difference in behavior observed for the CITED2 peptides with and without the LPEL and ϕC motifs suggests that the role of these regions is to drive the displacement of HIF-1α by CITED2.

Mechanistic Model from the NMR Data. The spectral behavior observed in the titration spectra for the CITED2 peptide variants is quite similar to the pattern of chemical shift and intensity changes observed for other IDP binding processes. For example, binding of the phosphorylated kinase-inducible domain

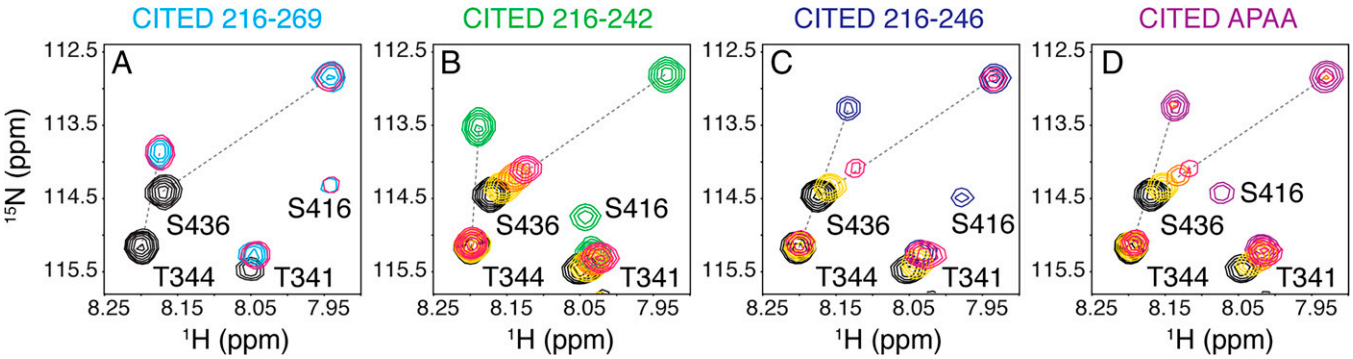

Fig. 4. NMR titrations provide mechanistic insight into competition between CITED2 and HIF-1α. Selected regions of superimposed ^{1}H-^{15}N HSQC spectra are shown for titration of CITED 216-269 (*A*), CITED 216-242 (*B*), CITED 216-246 (*C*), and CITED APAA (*D*) into a preformed complex of ^{15}N-TAZ1 and HIF-1α. In *A*, resonances corresponding to equimolar mixtures (1:1) of ^{15}N-TAZ1:HIF-1α and ^{15}N-TAZ1:CITED 216-269 are shown in black and light blue, respectively. Resonances corresponding to an equimolar mixture of ^{15}N-TAZ1, HIF-1α, and CITED 216-269 (1:1:1) are shown in magenta, with fewer contours displayed due to extreme overlap with ^{15}N-TAZ1:CITED 216-269 resonances. In *B–D*, resonances corresponding to an equimolar mixture (1:1) of ^{15}N-TAZ1:HIF-1α are shown in black, and resonances from samples containing ^{15}N-TAZ1 in the presence of one molar equivalent of HIF-1α and one, three, or five molar equivalents of CITED2 peptide are shown in gold, orange, and magenta, respectively. Resonances corresponding to the complexes of ^{15}N-TAZ1 bound to the CITED2 peptides are included for reference, with resonances for ^{15}N-TAZ1:CITED 216-242 in green (*B*), ^{15}N-TAZ1:CITED 216-246 in blue (*C*), and ^{15}N-TAZ1:CITED APAA in purple (*D*). In *C*, data are only shown for samples containing one and five molar equivalents of CITED 216-246. Spectra in *A* and *B* are reprinted with permission from ref. 16.

(pKID) of CREB to the ^{15}N-labeled KIX domain of CBP (24) proceeds by a multistep process, in which the IDP (pKID) initially engages the binding partner (^{15}N-KIX) through formation of an encounter complex before adopting the final lowest-energy bound state. A similar mechanism may also describe competition between HIF-1α and CITED2 for TAZ1 binding. At the simplest level, competition between HIF-1α and CITED2 could proceed in a two-state process, such that the effect of adding CITED2 to the TAZ1:HIF-1α complex would follow the reaction scheme:

$$\text{TAZ1:HIF-1}\alpha + \text{CITED2} \underset{k_{off}}{\overset{k_{on}}{\rightleftharpoons}} \text{TAZ1:CITED2} + \text{HIF-1}\alpha. \quad (1)$$

However, if CITED2 forms a ternary encounter complex with TAZ1 and HIF-1α, this reaction scheme would be expanded to include an additional step:

$$\text{TAZ1:HIF-1}\alpha + \text{CITED2} \underset{k_{-1}}{\overset{k_1}{\rightleftharpoons}} \text{TAZ1:HIF-1}\alpha\text{:CITED2} \underset{k_{-2}}{\overset{k_2}{\rightleftharpoons}} \text{TAZ1:CITED2} + \text{HIF-1}\alpha. \quad (2)$$

To discriminate between these two models, we carried out two-dimensional NMR line shape analysis of our NMR titration data for the variant CITED2 peptides using the program TITAN (25, 26). A simple two-state binding model (Scheme 1) is unable to reproduce the simultaneous changes in chemical shift and resonance intensity that are observed in our spectra as a function of increasing CITED2 peptide concentration (Fig. 5 and *SI Appendix*, Figs. S11–S13). While the two-state model described in Scheme 1 partially reproduces the changes in resonance intensity as a function of CITED2 peptide concentration for most residues included in our analysis, it does not reproduce the concentration-dependent chemical shift changes that are observed in the titration data, particularly for residues in the CITED2 αA binding site (see example data for S436 in Fig. 5). These results suggest that Scheme 1 is too minimal to describe competition between HIF-1α and CITED2.

Addition of a third state to the reaction mechanism as shown in Scheme 2 allows for robust simulation of the experimental data for all residues analyzed (Fig. 5 and *SI Appendix*, Figs. S11–S13 and Table S2). This analysis demonstrates unequivocally that competition between CITED2 and HIF-1α proceeds via an intermediate ternary complex. While the ^{15}N-TAZ1:HIF-1α:CITED2 ternary complex is not directly detectable in NMR experiments with the CITED 216-269 peptide, the NMR titration data for the truncated and mutated CITED2 peptides clearly reflect the presence of two processes: formation of the

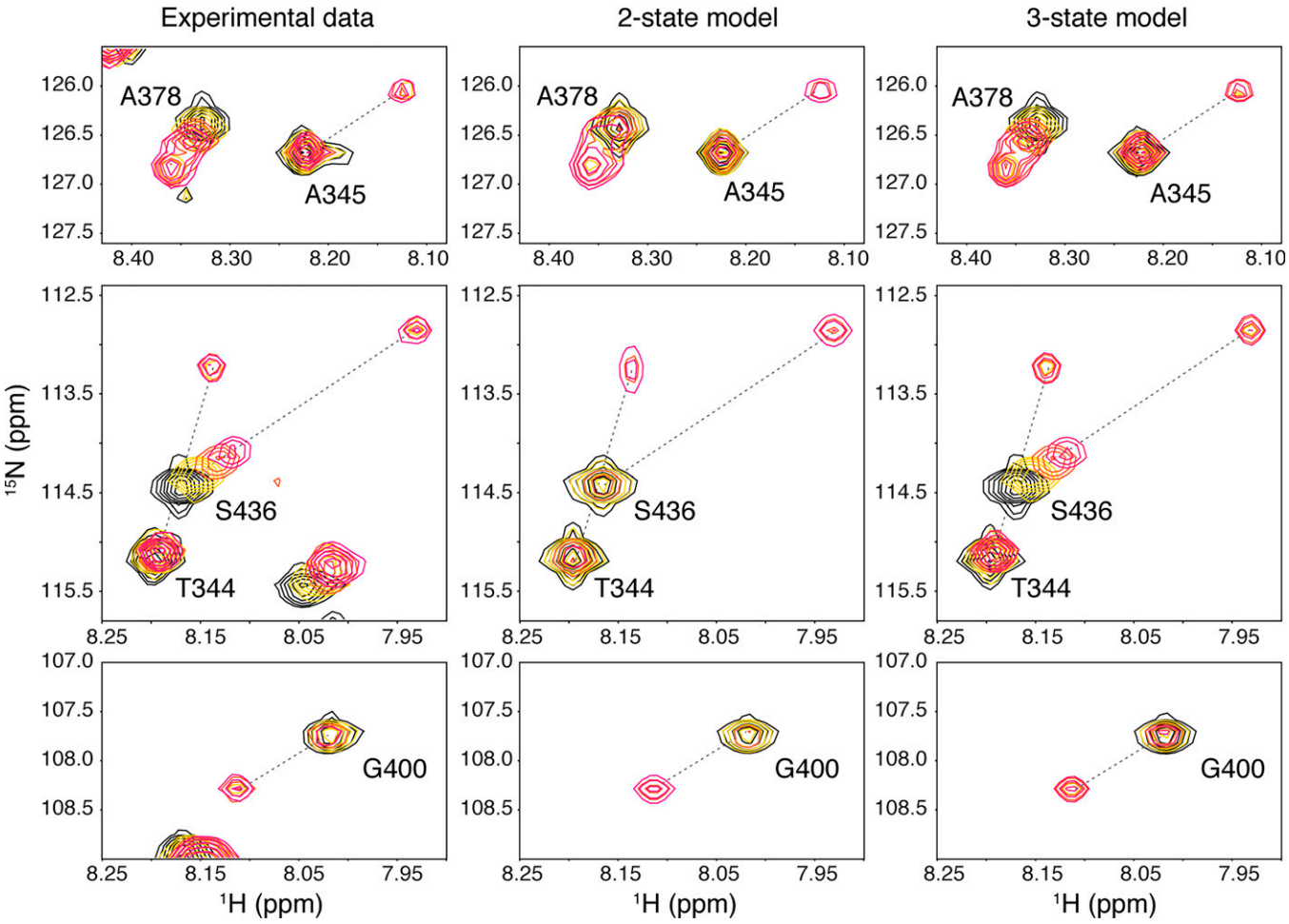

Fig. 5. NMR titration data can be described by a three-state model. (*Left*) Selected regions of the superimposed ^{1}H-^{15}N HSQC spectra for titration of the CITED APAA peptide into an NMR sample containing 100 μM of both ^{15}N-TAZ1 and HIF-1α. (*Center*) Selected regions of superimposed simulated spectra from TITAN analysis using a two-state binding model (Scheme 1). (*Right*) Selected regions of superimposed simulated spectra from TITAN analysis using a three-state binding model (Scheme 2). For all spectra, resonances corresponding to ^{15}N-TAZ1 bound to HIF-1α are shown in black, and resonances for samples containing equimolar amounts of ^{15}N-TAZ1 and HIF-1α as well as one, three, and five molar equivalents of the CITED APAA peptide are shown in gold, orange, and magenta, respectively.

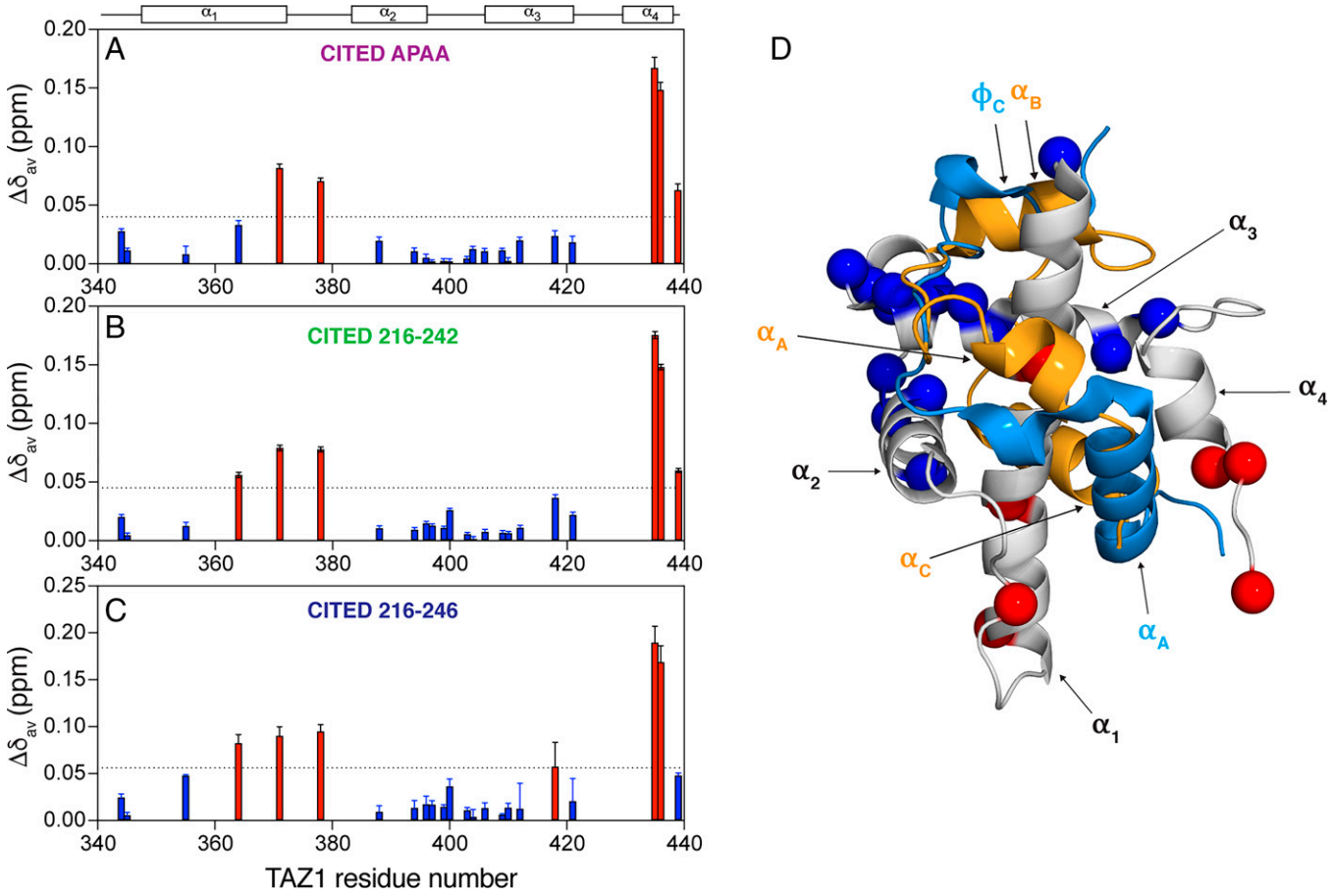

Fig. 6. NMR titrations provide structural insight into the TAZ1:HIF-1α:CITED2 ternary complex. (*A–C*) Weighted average chemical shift differences ($\Delta\delta_{av}$) between the intermediate state identified by TITAN line shape analysis (^{15}N-TAZ1 bound to both HIF-1α and CITED2 peptide) and ^{15}N-TAZ1 in complex with HIF-1α for the titration data with CITED APAA (*A*), CITED 216-242 (*B*), and CITED 216-246 (*C*) as a function of TAZ1 residue number. $\Delta\delta_{av}$ was calculated as $\Delta\delta_{av} = [(\Delta\delta_{HN})^2 + (\Delta\delta_N/5)^2]^{1/2}$. Data are shown for all TAZ1 residues analyzed. The dashed lines represent one SD above the 10% trimmed mean for the data shown, and residues with $\Delta\delta_{av}$ values above this cutoff are highlighted in red. (*D*) TAZ1 residues analyzed by line shape analysis are highlighted as spheres on the structure of TAZ1 (gray) bound to HIF-1α (orange; Protein Data Bank ID code 1L8C). The CITED2 transactivation domain (light blue) is superimposed onto the structure for reference (Protein Data Bank ID code1R8U). CITED2 residues 260 to 269 are omitted for clarity. Labels for structural elements and binding motifs are shown in black for TAZ1, orange for HIF-1α, and light blue for CITED2. TAZ1 residues that have $\Delta\delta_{av}$ values above the dashed lines in *A–C* are shown as red spheres; all other residues included in the line shape analysis are shown as blue spheres.

ternary complex (fast on the NMR timescale, corresponding to the first step in Scheme 2) and displacement of HIF-1α by CITED2 (slow on the NMR timescale). Line shape analysis enables estimation of the amide proton and nitrogen chemical shifts for the "invisible" intermediate state (*SI Appendix*, Table S1). For TAZ1 residues that contact the CITED2 N terminus and αA region, larger chemical shift differences are observed between the ternary intermediate and the ^{15}N-TAZ1:HIF-1α complex (Fig. 6, red bars and spheres), and the titration data show hallmarks of both fast and slow exchange processes (Fig. 4 *B–D*). However, for TAZ1 residues that contact the HIF-1α LPQL and αB motifs (also CITED2 LPEL and ϕC), the chemical shifts of the intermediate species are quite similar to the chemical shifts of the ^{15}N-TAZ1:HIF-1α complex (Fig. 6, blue bars and spheres), and only slow exchange behavior is observed (see example data for A345 and G400 in Fig. 5).

All CITED2 Motifs Are Required for Unidirectional Displacement of HIF-1α. Despite the critical insights gained from line shape analysis of the NMR titration data, we were limited in our ability to define the kinetic and thermodynamic parameters that describe the competition process. The fitted parameters from analyzing the data presented in Fig. 4 are poorly constrained (*SI Appendix*, Table S2), likely due to the narrow concentration range and limited number of titration points accessible in our NMR experiments. Nevertheless, the ability to model the titration data for the CITED2 peptide variants using the three-state model in Scheme 2 illustrates another important facet of competition between HIF-1α and CITED2 and suggests why different titration behavior is observed for CITED 216-269 relative to the truncated and mutated CITED2 peptides. CITED 216-269 competes with HIF-1α in a highly efficient, unidirectional manner, resulting in nearly irreversible displacement of HIF-1α and observation of only the CITED2 bound state by NMR (Fig. 4*A*) (16). In contrast, when key CITED2 binding motifs are missing, the NMR spectrum of ^{15}N-TAZ1:HIF-1α shows cross-peaks corresponding to the HIF-1α and CITED2 bound states as well as the ternary intermediate as the truncated and mutated CITED2 peptides are added, suggesting that loss of key CITED2 binding motifs may impact the reversibility of competition between HIF-1α and CITED2.

If the unidirectionality of competition is lost upon removal of key CITED2 binding motifs, then increasing the HIF-1α concentration should efficiently displace the CITED APAA and truncated CITED2 peptides from their complexes with TAZ1. This is confirmed in NMR titrations where the CITED APAA

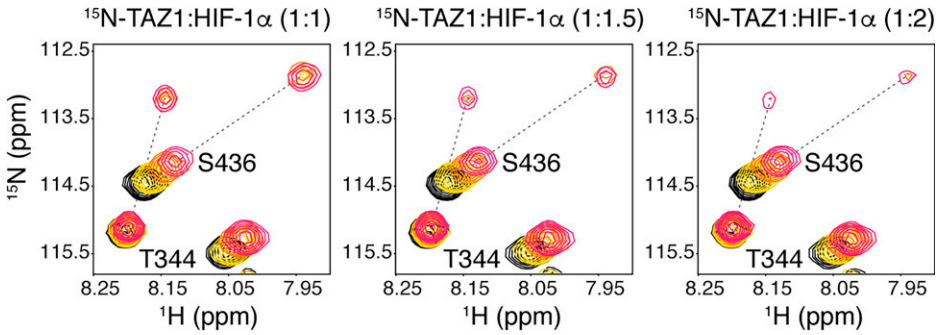

Fig. 7. Competition between HIF-1α and CITED APAA is fully reversible. Selected regions of superimposed ^{1}H-^{15}N HSQC spectra for titration of CITED APAA into mixtures of ^{15}N-TAZ1 and 1, 1.5, or 2 molar equivalents of HIF-1α as indicated above the spectra. In all spectra, resonances corresponding to the ^{15}N-TAZ1:HIF-1α complex are shown in black, and resonances from samples containing ^{15}N-TAZ1 in the presence of HIF-1α and one, three, or five molar equivalents of CITED APAA are shown in gold, orange, and magenta, respectively.

peptide is added to ^{15}N-TAZ1:HIF-1α samples that contain higher relative concentrations of HIF-1α. An increase in the HIF-1α concentration leads to a directly proportional increase in resonance intensity for the ^{15}N-TAZ1:HIF-1α bound state and a decrease in the intensity of resonances corresponding to the CITED2 complex (Fig. 7 and *SI Appendix*, Fig. S14). Reversibility of the competition between HIF-1α and CITED APAA is further confirmed by fluorescence anisotropy. Titration of HIF-1α into a preformed complex of Alexa594-labeled CITED APAA and TAZ1 shows that HIF-1α efficiently displaces CITED APAA, with a K_d^{app} that is unchanged from that of the binary TAZ1:HIF-1α complex (9 ± 2 nM) (*SI Appendix*, Fig. S15) (16). This is in sharp contrast to displacement of Alexa594-labeled CITED 216-269 from a preformed complex with TAZ1, which requires extremely high concentrations of HIF-1α (K_d^{app} = 0.9 ± 0.1 μM) (*SI Appendix*, Fig. S15) (16). Thus, we conclude that synergistic interactions involving all of the CITED2 binding motifs directly impact not only the efficiency of HIF-1α displacement but also the directionality and reversibility of the process.

Discussion

Many IDPs contain multiple binding motifs and participate in multivalent interactions that are critical to their diverse functional roles in the cell (1, 6, 27). The truncated and mutated CITED2 peptides studied here enable us to directly assess the contributions of discrete CITED2 interaction motifs to TAZ1 binding and competition with HIF-1α. CITED2 has three binding motifs that mediate interactions with TAZ1—the N-terminal αA region (which forms a stable α-helix in complex with TAZ1); the LPEL motif; and the adjacent ϕC motif, a highly conserved region containing hydrophobic and negatively charged amino acids (Fig. 1). Removal of both the LPEL and ϕC motifs has drastic effects on both binding and competition for TAZ1 (Figs. 2–4, Table 1, and *SI Appendix*, Figs. S1–S5). The CITED 216-242 peptide, which lacks the LPEL and ϕC motifs, is an extremely poor competitor against HIF-1α, with a K_d^{app} value more than three orders of magnitude larger than that of the full-length CITED2 activation domain (Figs. 3 and 4 and Table 1). The CITED APAA peptide, which retains the ϕC region but has a mutated LPEL motif, is also impaired in its ability to compete with HIF-1α, underscoring the importance of the LPEL motif in stabilizing the ternary intermediate and promoting HIF-1α dissociation. Deletion of the ϕC motif of CITED2 while retaining the LPEL motif, as in the CITED 216-246 peptide, also has pronounced effects on competition, suggesting that residues in the ϕC motif are important for stabilizing the interactions between CITED2 and TAZ1. Indeed, analysis of the picosecond-nanosecond (ps-ns) dynamics of the CITED 216-269 peptide in complex with TAZ1 (17) shows that many residues in the ϕC motif exhibit higher amide ^{15}N order parameters ($S^2 > 0.8$) than those of the nonproline residues of the LPEL motif ($S^2 = 0.76$), indicating greater motional restriction of the ϕC region on binding to TAZ1. These results emphasize the important role of the ϕC motif in stabilizing the TAZ1:CITED2 complex and increasing the efficiency with which CITED2 displaces bound HIF-1α.

Our results also show that the apparent unidirectionality of the competition between CITED2 and HIF-1α depends on which binding motifs of CITED2 are present. CITED2 is able to fully displace HIF-1α from its complex with TAZ1 at equimolar amounts, but extremely high concentrations of HIF-1α are required to compete with bound CITED2, resulting in a unidirectional, switch-like response (16). In contrast, our NMR titration experiments indicate that the truncated and mutated CITED2 peptides displace HIF-1α from the TAZ1 complex in a fully reversible manner; even a small increase in the HIF-1α concentration drives the equilibrium in Scheme 2 to the left and increases the intensity of ^{1}H-^{15}N HSQC cross-peaks corresponding to the ^{15}N-TAZ1:HIF-1α complex (Fig. 7 and *SI Appendix*, Fig. S14). This observation is supported by fluorescence anisotropy competition measurements (*SI Appendix*, Fig. S15), which show that HIF-1α efficiently displaces the mutated CITED APAA peptide from its complex with TAZ1 (K_d^{app} = 9 nM), whereas it is ineffective in displacing the unmutated CITED 216-269 (K_d^{app} = 900 nM) (16). In the NMR titrations, the intensities of resonances corresponding to both the ^{15}N-TAZ1:HIF-1α and ^{15}N-TAZ1:CITED2 variant peptide complexes reflect the relative populations expected based on the K_d^{app} values determined by fluorescence anisotropy (Figs. 3 and 4 and Table 1). In contrast, with the CITED 216-269 peptide, which retains all of the CITED2 binding motifs, only the ^{15}N-TAZ1:CITED 216-269 complex is observable when ^{15}N-TAZ1, HIF-1α, and CITED 216-269 are present in equimolar amounts, suggesting that the binding motifs of CITED2 function synergistically to drive displacement of HIF-1α.

Our data show that the CITED2 αA and LPEL motifs are not sufficient for unidirectional competition and point to interactions of the ϕC motif, which binds to the same site on TAZ1 as the HIF-1α αB helix, as a key driving force for unidirectionality. The backbone dynamics of CITED2 in the TAZ1 complex (17) strongly suggest that all three CITED2 binding motifs are thermodynamically coupled, allowing them to function in a highly cooperative manner to bind TAZ1 and prevent HIF-1α rebinding (16, 28). Binding of CITED2 to TAZ1 also promotes an allosteric conformational change in TAZ1 that disfavors binding of HIF-1α (16, 17). Recently, in an effort to characterize the ternary complex intermediate, we generated a CITED2/HIF-1α chimeric fusion peptide, in which the N-terminal region

of CITED2 (including the αA region and the LPEL motif) and the C-terminal region of HIF-1α (including the αB and αC helices) are linked in a single polypeptide chain to favor simultaneous interaction with TAZ1 (18). In solution, binding of the CITED2 αA and the HIF-1α αB–αC regions of the fusion peptide to TAZ1 is mutually exclusive; the HIF-1α region of the fusion peptide largely dominates the interactions with TAZ1 and destabilizes binding of CITED2 αA. This agrees extremely well with our findings in the current work; in the absence of stabilizing interactions between the ϕC motif of CITED2 and TAZ1, HIF-1α can readily compete with CITED2 for TAZ1 occupancy.

In conjunction with previous work (16–18), the present experiments provide insights into the mechanism by which the negative feedback regulator CITED2 facilitates unidirectional dissociation of HIF-1α from its complex with TAZ1. The NMR titrations with truncated and mutated CITED2 peptides confirm that competition between CITED2 and HIF-1α can be described, at minimum, by a three-state model (Scheme 2). The rate constants determined by line shape analysis indicate that the first step, binding of the CITED2 αA region to the TAZ1:-HIF-1α complex, is fast and reversible; TAZ1 cross-peaks associated with residues located in the CITED2 αA binding site shift in fast exchange toward their chemical shifts in the spectrum of the ternary intermediate (Figs. 4–6). Overall, the chemical shifts for the ternary intermediate closely resemble those for the ^{15}N-TAZ1:HIF-1α complex, except in regions that form the binding site for the CITED2 N terminus and αA region. Notably, the TAZ1 resonance positions of the ternary intermediate do not correspond to the CITED2-bound chemical shifts for any of the residues analyzed, indicating conformational differences in the binding site for the CITED2 αA region relative to the binary CITED2 complexes. In the ternary complex, HIF-1α remains anchored to TAZ1 through the αC helix and through interactions of the LPQL motif and αB. The chemical shifts of TAZ1 cross-peaks that report on interactions with the LPEL and ϕC motifs are unaffected by the fast process but undergo slow exchange changes in chemical shift upon displacement of HIF-1α (step 2 in Scheme 2). Thus, binding of CITED2 occurs by a sequential process; the αA helix of CITED2 binds rapidly to form a ternary complex in which the LPEL and ϕC motifs, which are strongly coupled to CITED2 αA, can compete efficiently, via an intramolecular process, with the HIF-1α LPQL and αB motifs for binding to TAZ1. As the CITED2:TAZ1 complex becomes progressively stabilized, binding of the HIF-1α αC helix is destabilized by allosteric conformational changes in TAZ1 (18), promoting complete dissociation of HIF-1α. In contrast to CITED2, the binding motifs in HIF-1α are connected by highly dynamic linkers and are only weakly coupled (17). After it is dissociated, HIF-1α cannot effectively rebind to displace CITED2 from its complex with TAZ1; binding of the HIF-1α αC helix is disfavored by the allosteric conformational change in TAZ1, while the weak thermodynamic coupling between the αC and αB regions renders the latter ineffective in competing with the ϕC motif of CITED2. This model is supported by molecular dynamics (MD) simulations, which show that the interaction motifs of CITED2 are strongly coupled and bind to TAZ1 in a highly cooperative manner, whereas the HIF-1α helices are uncoupled and bind noncooperatively to the TAZ1 domain (29).

Formation of a TAZ1:HIF-1α:CITED2 ternary complex that is on pathway for CITED2-driven displacement of HIF-1α from TAZ1 is consistent with our previous kinetics measurements that demonstrated formation of a ternary complex prior to HIF-1α dissociation (16). Similar multistep reaction mechanisms have been invoked for a number of IDPs as a hallmark of an "induced fit" mechanism for coupled folding and binding (3, 24). Detailed studies of IDP binding processes both in vitro and in silico (5, 30–32) have shown that the first step is often formation of an encounter complex, in which a single binding motif of the IDP participates in initial contacts with the binding partner before progression to the final bound state. Recently, several groups have carried out MD simulations to assess the molecular determinants of competition between HIF-1α and CITED2 (29, 33, 34). In all of the simulations, CITED2 forms a transient ternary complex with TAZ1 and HIF-1α that is on pathway for HIF-1α displacement. The CITED2 αA region and LPEL motif make favorable contacts with residues in the TAZ1 α1 and α4 helices and α1 and α3 helices, respectively, while HIF-1α remains partially bound to TAZ1 via its αC helix. A similar partially bound state of HIF-1α was identified in coarse-grained MD simulations of binary complex formation with TAZ1 (29, 34–36) and was also suggested by NMR relaxation dispersion experiments on the complex of hydroxylated HIF-1α and substoichiometric amounts of TAZ1 (37). Importantly, the ternary complex (or encounter complex) identified in the MD simulations shows the CITED2 LPEL motif bound to TAZ1. While our current experiments highlight the importance of the LPEL and ϕC motifs of CITED2 in modulating competition with HIF-1α, our data support a model for ternary complex formation in which CITED2 αA binding precedes binding of the LPEL and ϕC motifs. A sequential process for CITED2 αA and LPEL binding was observed in the simulations carried out by Chu et al. (33), where CITED2 αA binding precedes competition with HIF-1α for the shared LPQL/LPEL binding site, with exchange between the HIF-1α LPQL bound and the CITED2 LPEL bound states as the rate-limiting step for competition.

While binding of CITED2 αA and formation of the encounter complex are key steps in the competition process, the efficiency and apparent unidirectionality of competition between CITED2 and HIF-1α are clearly mediated through synergy of the CITED2 αA region with the LPEL and ϕC interaction motifs. Recent simulations suggested that the unidirectionality of the displacement process is predominantly determined by changes in electrostatic potential upon CITED2 binding that disfavor rebinding of HIF-1α (34). However, the Poisson Boltzmann electrostatic potential surfaces of the CITED2 and CITED APAA complexes are virtually identical, except for small differences in the immediate vicinity of the E245/A substitution (*SI Appendix*, Fig. S16), yet the APAA mutation renders the competition fully reversible (Fig. 7 and *SI Appendix*, Figs. S14 and S15). Our data thus provide strong evidence that synergistic binding of the thermodynamically coupled LPEL and ϕC motifs is a more potent driver of unidirectionality than are changes in the electrostatic potential.

These findings are also consistent with recent in vivo experiments (23). Using mouse models of retinal ischemic disease, we observed that the CITED 216-269 peptide is an extremely potent inhibitor of pathological angiogenesis caused by hypoxia and HIF transcriptional activation in the mouse eye, consistent with its behavior in vitro as a potent antagonist of HIF-1α. However, in the same models, the CITED APAA peptide was much less effective in down-regulating HIF-mediated transcription. In hypoxic tissues, HIF-1α would be continually produced and stabilized. Addition of CITED 216-269 would effectively prevent TAZ1 binding and transcriptional activation by HIF-1α. In contrast, HIF-1α would be able to effectively compete with the CITED APAA peptide, thus producing a damped regulatory response.

In conclusion, our data provide detailed mechanistic insight into the molecular determinants for facilitated displacement of one disordered protein by another on a shared binding partner. The flexibility and multivalency of the HIF-1α and CITED2 peptides enable efficient competition for binding to the TAZ1 domain of the transcriptional coactivator CBP. Synergistic interactions of

discrete but thermodynamically coupled CITED2 binding motifs are required for maintaining the directionality, fidelity, and efficiency of a critical transcriptional regulatory process. Our findings highlight the complexity of binding and competition processes involving disordered proteins and suggest that the prevalence of disorder in cellular signaling and biological regulation is an evolutionary advantage, enabling biological systems to circumvent the obstacles that would be encountered by stably folded interaction partners. As numerous intrinsically disordered regulatory proteins must compete for binding to limiting concentrations of CBP and p300 in the cell (7), it is anticipated that the complexity of the mechanism described here is likely to be relevant to many other facets of biology and disease.

Materials and Methods

Sample Preparation. The HIF-1α CTAD (human HIF-1α residues 776 to 826) and CITED2 CTAD (human CITED2 residues 216 to 269) peptides were expressed in *Escherichia coli* BL21 (DE3) containing the DNAY plasmid, as coexpressions with TAZ1 (mouse CBP residues 340 to 439) and purified by nickel affinity chromatography and reversed-phase high-performance liquid chromatography (HPLC) as described previously (16). The plasmids encoding the truncated and mutated CITED2 peptides (also coexpressed with TAZ1) were generated by standard mutagenesis protocols, and the peptides were prepared in the same manner as the full-length CITED2 transactivation domain peptide. The HIF-1α peptide includes an additional four nonnative residues at the N terminus (GSHM), and the CITED2 peptides include an additional five residues at the N terminus (GSHMS). TAZ1 was expressed and purified under native conditions as described previously, with uniform ^{15}N labeling achieved using [^{15}N]-ammonium chloride (0.5 g/L) and [^{15}N]-ammonium sulfate (0.5 g/L) as the sole nitrogen sources (16). The identity and purity of all proteins were confirmed by mass spectrometry.

Lyophilized HIF-1α and CITED2 peptides were reconstituted in 50 mM Tris(hydroxymethyl)aminomethane (Tris), pH 8, with 10 mM fresh dithiothreitol (DTT) and dialyzed into buffer containing 20 mM Tris·HCl, pH 6.8, 50 mM NaCl, and 2 mM DTT. TAZ1 samples were also dialyzed into the same buffer for all experiments. Protein sample concentrations were determined by ultraviolet (UV) absorbance at 280 nm using extinction coefficients calculated using the ExPASy ProtParam web server (38). For protein samples that lack tyrosine and tryptophan residues, concentrations were determined by UV absorbance at 205 nm (39).

NMR Experiments. All NMR samples were prepared in buffer containing 20 mM Tris·HCl, pH 6.8, 50 mM NaCl, 2 mM DTT, and 5% D_2O. For all samples, the concentration of the labeled component (^{15}N-TAZ1) was 100 μM. NMR samples for the ^{15}N-TAZ1:HIF-1α and ^{15}N-TAZ1:CITED 216-269 complexes were prepared as equimolar mixtures (100 μM of each component). Samples for the complexes of ^{15}N-TAZ1 with the truncated and mutated CITED2 peptides, which bind more weakly, were prepared with a 1:5 molar ratio of ^{15}N-TAZ1:-CITED2 peptide (100 μM ^{15}N-TAZ1 and 500 μM CITED2 peptide). NMR data were collected at 298 K on a Bruker Avance 900-MHz spectrometer. Data were processed using NMRPipe (40) and analyzed using NMRFAM-SPARKY (41) on the NMRbox platform (42).

Fluorescence Anisotropy. All fluorescence measurements were carried out on an ISS PC1 photon counting fluorimeter at 298 K in buffer containing 20 mM Tris·HCl, pH 6.8, 50 mM NaCl, and 2 mM DTT. Alexa594-labeled HIF-1α peptides (with a C800V mutation introduced to ensure single-site labeling at C780) were prepared as previously described (16). The CITED 216-269 and CITED APAA peptides were labeled with Alexa594 dye in a similar manner at C261 in the disordered C-terminal region. For competition assays, unlabeled CITED2 or HIF-1α peptides were titrated into preformed complexes of 20 nM Alexa594–HIF-1α, Alexa594–CITED 216-269, or Alexa594–CITED2 APAA and 250 nM TAZ1. K_d^{app} values were determined from nonlinear least squares fitting to a competitive binding model (43–45) using GraphPad Prism 8 (GraphPad Software, Inc.).

NMR Titrations and Line Shape Analysis. NMR samples for titrations were prepared by mixing ^{15}N-TAZ1, HIF-1α, and CITED2 peptides that had been dialyzed into identical buffers containing 20 mM Tris·HCl, pH 6.8, 50 mM NaCl, 2 mM DTT, and 5% D_2O. For titrations, NMR samples containing equimolar ratios of ^{15}N-TAZ1 and HIF-1α (100 μM each) were prepared with one (100 μM) and five (500 μM) molar equivalents of CITED 216-269, CITED 216-246, CITED 216-242, or CITED APAA peptide. Samples of ^{15}N-TAZ1 and HIF-1α in the presence of three molar equivalents (300 μM) of the CITED2 peptides were then prepared by mixing the samples with one and five molar equivalents of the CITED2 peptides in equal amounts. Similar titrations were also carried out with NMR samples containing mixtures of 100 μM ^{15}N-TAZ1 and 150 or 200 μM HIF-1α, with 100 or 500 μM CITED APAA added. Samples of ^{15}N-TAZ1 and HIF-1α in the presence of 300 μM CITED APAA were then prepared by mixing the samples with 100 and 500 μM CITED APAA in equal amounts. ^{1}H-^{15}N HSQC spectra were also acquired for samples of ^{15}N-TAZ1:HIF-1α and ^{15}N-TAZ1:CITED2 peptide complexes over the entire concentration series under the same conditions for direct comparison with the titration spectra.

For two-dimensional NMR line shape analysis, the ^{1}H-^{15}N HSQC spectra were processed using exponential window functions with 4-Hz line broadening in the direct dimension and 8-Hz line broadening in the indirect dimension. The spectra were imported into TITAN (25, 26) and analyzed using the "two-state" and "ligand exchange via ternary complex" binding models. Line shape analysis was carried out in two steps, in which the chemical shifts and line widths of the ^{15}N-TAZ1:HIF-1α bound state were determined first, followed by subsequent fitting of the chemical shifts and line widths of the intermediate and bound states and kinetic parameters for the binding models. Twenty-three well-resolved ^{15}N-TAZ1 resonances were included in the analysis, and errors were estimated using bootstrap resampling (100 replicas).

Data Availability. All study data are included in the article and/or *SI Appendix*.

ACKNOWLEDGMENTS. We thank Gerard Kroon for assistance with NMR experiments, Euvel Manlapaz for technical assistance, Ashok Deniz for fluorimeter access, and Maria Martinez-Yamout and Frank Appling for many helpful discussions. This work was supported by NIH Grants GM131693 (to H.J.D.), CA096865 (to P.E.W.), and CA229652 (to P.E.W.) and by the Skaggs Institute of Chemical Biology. R.B.B. was supported by American Cancer Society Postdoctoral Fellowship 125343-PF-13-202-01-DMC.

1. P. E. Wright, H. J. Dyson, Intrinsically disordered proteins in cellular signalling and regulation. *Nat. Rev. Mol. Cell Biol.* **16**, 18–29 (2015).
2. M. Arai, Unified understanding of folding and binding mechanisms of globular and intrinsically disordered proteins. *Biophys. Rev.* **10**, 163–181 (2018).
3. R. B. Berlow, H. J. Dyson, P. E. Wright, Functional advantages of dynamic protein disorder. *FEBS Lett.* **589**, 2433–2440 (2015).
4. H.-X. Zhou, P. A. Bates, Modeling protein association mechanisms and kinetics. *Curr. Opin. Struct. Biol.* **23**, 887–893 (2013).
5. L. Mollica *et al.*, Binding mechanisms of intrinsically disordered proteins: Theory, simulation, and experiment. *Front. Mol. Biosci.* **3**, 52 (2016).
6. R. B. Berlow, H. J. Dyson, P. E. Wright, Expanding the paradigm: Intrinsically disordered proteins and allosteric regulation. *J. Mol. Biol.* **430**, 2309–2320 (2018).
7. R. H. Goodman, S. Smolik, CBP/p300 in cell growth, transformation, and development. *Genes Dev.* **14**, 1553–1577 (2000).
8. G. A. Blobel, CREB-binding protein and p300: Molecular integrators of hematopoietic transcription. *Blood* **95**, 745–755 (2000).
9. A. Giordano, M. L. Avantaggiati, p300 and CBP: Partners for life and death. *J. Cell. Physiol.* **181**, 218–230 (1999).
10. D. C. Bedford, L. H. Kasper, T. Fukuyama, P. K. Brindle, Target gene context influences the transcriptional requirement for the KAT3 family of CBP and p300 histone acetyltransferases. *Epigenetics* **5**, 9–15 (2010).
11. H. J. Dyson, P. E. Wright, Role of intrinsic protein disorder in the function and interactions of the transcriptional coactivators CREB-binding protein (CBP) and p300. *J. Biol. Chem.* **291**, 6714–6722 (2016).
12. Z. Arany *et al.*, An essential role for p300/CBP in the cellular response to hypoxia. *Proc. Natl. Acad. Sci. U.S.A.* **93**, 12969–12973 (1996).
13. S. Bhattacharya *et al.*, Functional role of p35srj, a novel p300/CBP binding protein, during transactivation by HIF-1. *Genes Dev.* **13**, 64–75 (1999).
14. P. J. Kallio *et al.*, Signal transduction in hypoxic cells: Inducible nuclear translocation and recruitment of the CBP/p300 coactivator by the hypoxia-inducible factor-1α. *EMBO J.* **17**, 6573–6586 (1998).
15. J. Gu, J. Milligan, L. E. Huang, Molecular mechanism of hypoxia-inducible factor 1α-p300 interaction. A leucine-rich interface regulated by a single cysteine. *J. Biol. Chem.* **276**, 3550–3554 (2001).
16. R. B. Berlow, H. J. Dyson, P. E. Wright, Hypersensitive termination of the hypoxic response by a disordered protein switch. *Nature* **543**, 447–451 (2017).
17. R. B. Berlow, M. A. Martinez-Yamout, H. J. Dyson, P. E. Wright, Role of backbone dynamics in modulating the interactions of disordered ligands with the TAZ1 domain of the CREB-binding protein. *Biochemistry* **58**, 1354–1362 (2019).
18. F. D. Appling, R. B. Berlow, R. L. Stanfield, H. J. Dyson, P. E. Wright, The molecular basis of allostery in a facilitated dissociation process. *Structure* **29**, 1327–1338 (2021).

19. S. A. Dames, M. Martinez-Yamout, R. N. De Guzman, H. J. Dyson, P. E. Wright, Structural basis for Hif-1α /CBP recognition in the cellular hypoxic response. *Proc. Natl. Acad. Sci. U.S.A.* **99**, 5271–5276 (2002).
20. S. J. Freedman *et al.*, Structural basis for recruitment of CBP/p300 by hypoxia-inducible factor-1α. *Proc. Natl. Acad. Sci. U.S.A.* **99**, 5367–5372 (2002).
21. R. N. De Guzman, M. A. Martinez-Yamout, H. J. Dyson, P. E. Wright, Interaction of the TAZ1 domain of the CREB-binding protein with the activation domain of CITED2: Regulation by competition between intrinsically unstructured ligands for non-identical binding sites. *J. Biol. Chem.* **279**, 3042–3049 (2004).
22. S. J. Freedman *et al.*, Structural basis for negative regulation of hypoxia-inducible factor-1α by CITED2. *Nat. Struct. Biol.* **10**, 504–512 (2003).
23. A. Usui-Ouchi *et al.*, An allosteric peptide inhibitor of HIF-1α regulates hypoxia-induced retinal neovascularization. *Proc. Natl. Acad. Sci. U.S.A.* **117**, 28297–28306 (2020).
24. K. Sugase, H. J. Dyson, P. E. Wright, Mechanism of coupled folding and binding of an intrinsically disordered protein. *Nature* **447**, 1021–1025 (2007).
25. C. A. Waudby, A. Ramos, L. D. Cabrita, J. Christodoulou, Two-dimensional NMR lineshape analysis. *Sci. Rep.* **6**, 24826 (2016).
26. C. A. Waudby, J. Christodoulou, NMR lineshape analysis of intrinsically disordered protein interactions. *Methods Mol. Biol.* **2141**, 477–504 (2020).
27. H. Y. J. Fung, M. Birol, E. Rhoades, IDPs in macromolecular complexes: The roles of multivalent interactions in diverse assemblies. *Curr. Opin. Struct. Biol.* **49**, 36–43 (2018).
28. H. N. Motlagh, J. Li, E. B. Thompson, V. J. Hilser, Interplay between allostery and intrinsic disorder in an ensemble. *Biochem. Soc. Trans.* **40**, 975–980 (2012).
29. I. Ruiz-Ortiz, D. De Sancho, Competitive binding of HIF-1α and CITED2 to the TAZ1 domain of CBP from molecular simulations. *Phys. Chem. Chem. Phys.* **22**, 8118–8127 (2020).
30. G. J. Gerlach, R. Carrock, R. Stix, E. J. Stollar, K. A. Ball, A disordered encounter complex is central to the yeast Abp1p SH3 domain binding pathway. *PLoS Comput. Biol.* **16**, e1007815 (2020).
31. G. Schreiber, G. Haran, H. X. Zhou, Fundamental aspects of protein-protein association kinetics. *Chem. Rev.* **109**, 839–860 (2009).
32. H. X. Zhou, Intrinsic disorder: Signaling via highly specific but short-lived association. *Trends Biochem. Sci.* **37**, 43–48 (2012).
33. W.-T. Chu, X. Chu, J. Wang, Investigations of the underlying mechanisms of HIF-1α and CITED2 binding to TAZ1. *Proc. Natl. Acad. Sci. U.S.A.* **117**, 5595–5603 (2020).
34. Y. Wang, C. L. Brooks III, Electrostatic forces control the negative allosteric regulation in a disordered protein switch. *J. Phys. Chem. Lett.* **11**, 864–868 (2020).
35. D. Ganguly, W. Zhang, J. Chen, Electrostatically accelerated encounter and folding for facile recognition of intrinsically disordered proteins. *PLoS Comput. Biol.* **9**, e1003363 (2013).
36. D. De Sancho, R. B. Best, Modulation of an IDP binding mechanism and rates by helix propensity and non-native interactions: Association of HIF1α with CBP. *Mol. Biosyst.* **8**, 256–267 (2012).
37. K. Sugase, J. C. Lansing, H. J. Dyson, P. E. Wright, Tailoring relaxation dispersion experiments for fast-associating protein complexes. *J. Am. Chem. Soc.* **129**, 13406–13407 (2007).
38. E. Gasteiger *et al.*, "Protein identification and analysis tools on the ExPASy server" in *The Proteomics Protocols Handbook*, J. M. Walker, Ed. (Springer Protocols Handbooks, Humana Press, Totowa, NJ, 2005), pp. 571–607.
39. N. J. Anthis, G. M. Clore, Sequence-specific determination of protein and peptide concentrations by absorbance at 205 nm. *Protein Sci.* **22**, 851–858 (2013).
40. F. Delaglio *et al.*, NMRPipe: A multidimensional spectral processing system based on UNIX pipes. *J. Biomol. NMR* **6**, 277–293 (1995).
41. W. Lee, M. Tonelli, J. L. Markley, NMRFAM-SPARKY: Enhanced software for biomolecular NMR spectroscopy. *Bioinformatics* **31**, 1325–1327 (2015).
42. M. W. Maciejewski *et al.*, NMRbox: A resource for biomolecular NMR computation. *Biophys. J.* **112**, 1529–1534 (2017).
43. Z. X. Wang, An exact mathematical expression for describing competitive binding of two different ligands to a protein molecule. *FEBS Lett.* **360**, 111–114 (1995).
44. M. H. Roehrl, J. Y. Wang, G. Wagner, A general framework for development and data analysis of competitive high-throughput screens for small-molecule inhibitors of protein-protein interactions by fluorescence polarization. *Biochemistry* **43**, 16056–16066 (2004).
45. C. W. Lee, J. C. Ferreon, A. C. Ferreon, M. Arai, P. E. Wright, Graded enhancement of p53 binding to CREB-binding protein (CBP) by multisite phosphorylation. *Proc. Natl. Acad. Sci. U.S.A.* **107**, 19290–19295 (2010).